

Article

Evaluating the Atmospheric Loss of H₂ by NO₃ Radicals: A Theoretical Study

Manolis N. Romanias^{1,*}  and Thanh Lam Nguyen^{2,*} 

¹ Institute Mines-Télécom Nord Europe, Center for Energy and Environment, University of Lille, F-59000 Lille, France

² Quantum Theory Project, Departments of Chemistry and Physics, University of Florida, Gainesville, FL 32611, USA

* Correspondence: emmanouil.romanias@imt-nord-europe.fr (M.N.R.); tlam.nguyen@chem.ufl.edu (T.L.N.)

Abstract: Molecular hydrogen (H₂) is now considered among the most prominent substitute for fossil fuels. The environmental impacts of a hydrogen economy have received more attention in the last years, but still, the knowledge is relatively poor. In this work, the reaction of H₂ with NO₃ radical (the dominant night-time detergent of the atmosphere) is studied for the first time using high-level composite G3B3 and modification of high accuracy extrapolated ab initio thermochemistry (mHEAT) methods in combination with statistical kinetics analysis using non-separable semi-classical transition state theory (SCTST). The reaction mechanism is characterized, and it is found to proceed as a direct H-abstraction process to yield HNO₃ plus H atom. The reaction enthalpy is calculated to be 12.8 kJ mol⁻¹, in excellent agreement with a benchmark active thermochemical tables (ATcT) value of 12.2 ± 0.3 kJ mol⁻¹. The energy barrier of the title reaction was calculated to be 74.6 and 76.7 kJ mol⁻¹ with G3B3 and mHEAT methods, respectively. The kinetics calculations with the non-separable SCTST theory give a modified-Arrhenius expression of $k(T) = 10^{-15} \times T^{0.7} \times \exp(-6120/T)$ (cm³ s⁻¹) for T = 200–400 K and provide an upper limit value of 10⁻²² cm³ s⁻¹ at 298 K for the reaction rate coefficient. Therefore, as compared to the main consumption pathway of H₂ by OH radicals, the title reaction plays an unimportant role in H₂ loss in the Earth's atmosphere and is a negligible source of HNO₃.

Keywords: kinetics; CFOUR; SCTST; H₂ fuel; NO₃



Citation: Romanias, M.N.; Nguyen, T.L. Evaluating the Atmospheric Loss of H₂ by NO₃ Radicals: A Theoretical Study. *Atmosphere* **2022**, *13*, 1313. <https://doi.org/10.3390/atmos13081313>

Academic Editors: Kazimierz Gaj and Robert Oleniacz

Received: 26 July 2022

Accepted: 14 August 2022

Published: 18 August 2022

Publisher's Note: MDPI stays neutral with regard to jurisdictional claims in published maps and institutional affiliations.



Copyright: © 2022 by the authors. Licensee MDPI, Basel, Switzerland. This article is an open access article distributed under the terms and conditions of the Creative Commons Attribution (CC BY) license (<https://creativecommons.org/licenses/by/4.0/>).

1. Introduction

Climate change and air pollution are key challenges that our society is currently facing. The growing average temperature of the planet leads to the increased frequency of extreme climatic events such as heat/cold waves, floods, periods of drought, and so on. According to the latest Intergovernmental Panel on Climate Change (IPCC) report [1], if no action is taken, the consequences for our planet and society will be catastrophic [1]. In addition, air pollution is also a major environmental problem, which causes millions of deaths each year [2]. Both climate change and air pollution are related to intensive anthropogenic activities through the combustion of fossil fuels. To limit climate change and improve air quality, the world is preparing for a transition from fossil-fuel-based energy systems to renewable energy sources. Among the different technologies proposed, a hydrogen economy has received particular attention [3,4]. The feasibility of a hydrogen economy is still under question, mainly due to the potential environmental impacts, the security of the energy supply, the cost of energy production, etc. [5–9].

The current atmospheric levels of H₂ vary from 400 to 550 ppb with a seasonal variability observed in both hemispheres of the Earth [10,11]. H₂ sources are estimated to range between 30 to 107 Tg per year, with the latest estimation being 41 ± 11 Tg per year [10], mostly coming from the photochemical degradation of volatile organic compounds (VOCs),

methane (CH₄), and isoprene (C₅H₈) [10,11]. Fossil fuel combustion and biomass burning are also important contributors [10]. Interestingly, recently, Patterson et al. reconstructed the atmospheric profiles of H₂ and evidenced a correlation between H₂ atmospheric compositions with combustion processes, induced by anthropogenic activities after the industrial revolution [12].

Dry deposition is considered the major sink of atmospheric hydrogen [10]. The dry deposition velocities were calculated to be in the range of 0.01 to 0.11 cm s⁻¹, and thus dry deposition may account for up to 80% of H₂ removal. H₂ can be also removed from the atmosphere, through reaction with the major atmospheric oxidants [10]. In particular, the reaction of H₂ with OH radicals has been determined as an important sink:



with $\Delta_r H^\circ$ (298 K) = -61.2 kJ mol⁻¹ [13], k_1 (298 K) = 6.7×10^{-15} cm⁻³ molecule⁻¹ s⁻¹ [14].

H₂ can also react with Cl atoms leading to HCl formation:



Although the reaction (R2) is endothermic, $\Delta_r H^\circ$ (298 K) = 4.4 kJ mol⁻¹ [13], the corresponding rate coefficient is k_2 (298K) = 1.5×10^{-14} cm⁻³ molecule⁻¹ s⁻¹ [14], thus being about two times faster than that of the reaction (R1). Nevertheless, the average concentrations of Cl atoms in the troposphere are three orders of magnitude lower than that of OH; as a result, reaction (R1) dominates. Cl chemistry could be important in coastal areas where Cl atmospheric concentrations are significantly higher [15,16].

The atmospheric/climatic impacts because of a wide range of applications of H₂-based technologies have received more attention in the last decades. Until today, one of the most challenging aspects of a hydrogen economy is H₂ leaks. Therefore, different scenarios have been developed based on (a) the energy demand that will be covered with the application of H₂ technology and (b) an estimated percentage of H₂ released in the atmosphere due to leaks during storage and transportation. On the global scale, H₂ concentrations are predicted to increase by 20% up to 2.5 times depending on different scenarios [5,9].

The impact of H₂ increases on a regional scale (due to an accidental massive release of H₂) has not been evaluated yet. Literature studies have shown that increased tropospheric levels of H₂ can indirectly influence the atmospheric lifetime of CH₄, the second most important greenhouse gas in the atmosphere [8]. Indeed, the documented reaction rate coefficients of OH radicals (the major tropospheric oxidant) with H₂ (R1) and CH₄ (R3) (with k_3 (298 K) = 6.3×10^{-15} cm⁻³ molecule⁻¹ s⁻¹ [14]) are comparable:



Consequently, the increase in H₂ can break down the future goals for the reduction in CH₄, and possibly, it could increase CH₄ in the stratosphere. Therefore, a progressive increase in H₂ concentration could impact the oxidative capacity of the atmosphere and indirectly impact the tropospheric lifetime of long-lived species. Other climatic impacts of a H₂ increase are related to an increase in water concentrations and ozone (O₃) in the stratosphere, resulting in increasing coverage of polar stratospheric clouds (PSC) [9]. Heterogeneous processes in PSCs are responsible for the Antarctica ozone hole [17].

Certainly, our current state of knowledge about the impacts of an increase in H₂ in the atmosphere is limited and needs to be further evaluated. In the framework of the current study, we aim to investigate for the first time in the literature the impact of H₂ reaction with NO₃ radicals:



(R4) is an endothermic reaction, $\Delta_r H^\circ$ (298 K) = 10.4 kJ mol⁻¹ [13]. However, like reaction (R2), this does not preclude that it cannot occur under relevant tropospheric conditions. NO₃ is the dominant tropospheric oxidant during nighttime and plays a

crucial role in the oxidative capacity of the troposphere, regulating the lifetime of many atmospheric species [18,19]. The average NO₃ concentrations are around two orders of magnitude greater than those of OH radicals [16]. Furthermore, nitric acid (HNO₃), a product of the reaction (R4), is an important atmospheric compound, e.g., it regulates the atmospheric acidity of the troposphere and participates in a series of heterogeneous reactions that influences air quality and climate [20,21]. It is, therefore, fundamental to study the potential impact of the reaction (R4) in the atmosphere. We applied high-level quantum chemical calculations and the non-separable SCTST theory to determine the temperature-dependent k_4 and to evaluate the atmospheric contribution of the reaction (R4).

2. Theoretical Methodologies

2.1. Quantum Chemical Calculations

First, electronic structure calculations of the title reaction were performed using the Gaussian 16 program suite [22]. The calculations were carried out using the composite G3B3 method [23], which is a variation of the G3 theory [24]. This multipart method consists of geometry optimization and vibrational frequency calculations at the B3LYP/6-31G(d) level of theory [25]. Thereafter, a series of single-point energy calculations at four different levels of theory including QCISD(T)/6-31G(d), MP4/6-31 + G(d), MP4/6-31G(2df,p), and MP2/G3Large were accomplished. Intrinsic reaction coordinate (IRC) calculations were also performed to verify that the located transition state (TS) structures are connecting to the proper reactants and products.

It should be mentioned that NO₃ is a typical difficult molecule for quantum chemical calculation [26]. For NO₃, the B3LYP calculations give a C_{2v} point group, although the experimentally determined ground state average geometry is D_{3h}. Although a comparison of equilibrium geometries with experimental structures is fraught with difficulties, especially for a system of this type, the potential surface for NO₃ near the minimum is very flat. Hence, many methods give correct symmetric structures while many others give broken symmetry structures. However, the energetics are largely insensitive to its symmetry, owing to the flatness of the surface.

To provide a high accuracy barrier for the later kinetics calculations, in addition to the G3B3 method, high-level coupled-cluster calculations with the mHEAT-345(Q) method have been employed as well [27]. mHEAT is also a composite method, which is mainly based on the CCSD(T) calculations to obtain optimized structures, rovibrational parameters, anharmonic zero-point vibrational energies (ZPE), and electron correlations. To achieve high accuracy of 1–2 kJ mol^{−1} for the barrier and the reaction enthalpy, higher level corrections—which go beyond the CCSD(T)—including fully triple and non-iterative quadruple excitations were also considered. The CFOUR quantum chemical program was used for the mHEAT calculations [28].

2.2. Statistical Kinetics Calculations

The title reaction undergoes a direct H-abstraction leading to products (HNO₃ + H) without passing through an energized intermediate/adduct, so it does not depend on pressure. Therefore, the reaction rate constants can be computed at the high-pressure limit (e.g., when the Boltzmann thermal energy distribution is fully established) using non-separable semi-classical transition state theory (SCTST) [29–33]:

$$k_{\infty}(T) = \frac{\sigma}{h} \times \frac{Q_{tr}^{\ddagger} Q_e^{\ddagger}}{Q_{H_2}^{re} \cdot Q_{NO_3}^{re}} \times \sum_{J=0}^{\infty} (2J+1) \int_0^{\infty} G_{rv}^{\ddagger}(E, J) \times \exp(-E/k_B T) dE, \quad (1)$$

Here, T is the reaction temperature, and E is the total internal energy. k_B is Boltzmann's constant, h is Planck's constant, and $\sigma = \frac{\sigma_{H_2} \cdot \sigma_{NO_3}}{\sigma_{TS}} = 12$ is the reaction path degeneracy. It should be noted that the rotational symmetry numbers for H₂, NO₃, and the TS are 2, 6, and 1, respectively. $Q_{H_2}^{re}$ and $Q_{NO_3}^{re}$ are the complete partition functions for H₂ and NO₃,

respectively, but without the symmetry numbers in the rotational partition functions of H₂ and NO₃. Q_{tr} is the translational partition function, and Q_e is the electronic partition function of the TS (the superscripts “re” and “≠” designate reactants and transition state (TS), respectively). Electronic partition functions for all stationary points are equal to 2 for a doublet electronic state and 1 for a singlet electronic state. G_{rv}^{\neq} is the sum of rovibrational quantum states of the TS for the given E and J , which can be obtained from its vibrational counterpart using the J -shifting approximation [34–36], Equation (2):

$$G_{rv}^{\neq}(E, J) = \sum_{K=-J}^{K=+J} G_v^{\neq}(E - E_r(J, K)) \quad (2a)$$

$$\rho_{rv}(E, J) = \sum_{K=-J}^{K=+J} \rho_v(E - E_r(J, K)) \quad (2b)$$

In Equation (2), G_v^{\neq} is the anharmonic (coupled) vibrational sum of states of the TS that is calculated using Miller’s semi-classical TST (SCTST) theory [29–33] based on the Wang–Landau algorithm [32,37–39]. SCTST theory [29–31,33,40] automatically includes coupled anharmonic vibrations and multi-dimensional quantum mechanical tunneling. E_r is the (external) rotational energy level of the TS, which is approximated by a symmetric top [41], Equation (3):

$$E_r(J, K) = J(J + 1)\bar{B} + (A - \bar{B})K^2, \text{ with } \bar{B} = \sqrt{B \cdot C} \text{ and } -J \leq K \leq +J \quad (3)$$

It should be mentioned that the calculated rate coefficients in this case may be off by a factor of 2.

3. Results and Discussion

Reaction Mechanisms and Energetics

The reaction of NO₃ radical with H₂ proceeds through a direct H-abstraction step to yield HNO₃ and H atom (see Figure 1). This reaction pathway has to surmount a barrier height of 74.6 and 76.7 kJ mol^{−1} calculated by the G3B3 and mHEAT methods, respectively. Individual contributions of various terms to the total energy barrier of TS were given in Table 1. As seen there, the SCF calculations—which do not include electron correlation—are incorrect because they give an unphysical negative barrier of −10.9 kJ mol^{−1}. The most important contribution to the energy barrier is 81.6 kJ mol^{−1}, coming from the electron correlation obtained with the CCSD(T) calculations. The ZPE correction is moderate with a value of 2.9 kJ mol^{−1}. Including the T(T) and (Q)-T corrections is also important to achieve an accuracy of 2 kJ mol^{−1}, and they have opposite signs in this case. The endothermicity of the reaction at 0 K calculated with the G3B3 method is 12.8 kJ mol^{−1}, which agrees well with a benchmark ATcT value of 12.2 ± 0.3 kJ mol^{−1} [13]. The G3B3 theory shown earlier can provide accurate thermochemical parameters of NO₃ radical reactions [42]. The optimized geometries and rovibrational parameters of reactants, products, and the transition state are given in the Supplementary Material. It should be noted that the calculated relative energies in Figure 1 include zero-point energy corrections. We could not find the formation of a pre-reactive complex or a post-product complex. Another possible limitation that is not considered in this work is to carry out fully dynamics (scattering) calculations on a (locally) global PES, which is constructed using the full-CI method. However, such calculations are unpractical because of the size of the system.

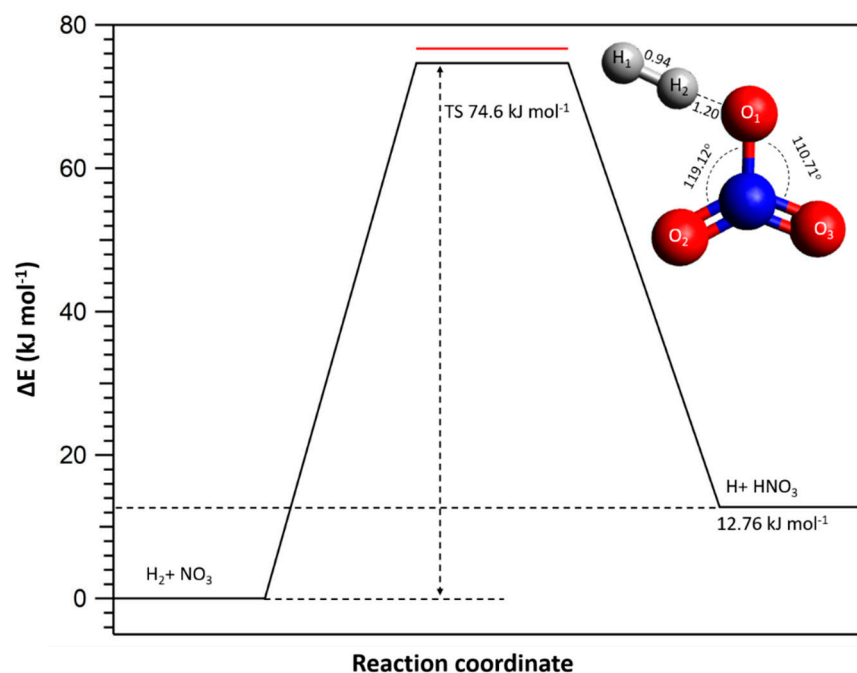


Figure 1. Schematic reaction energy profile for the reaction of NO_3 radical with H_2 calculated using the G3B3 (in black) and mHEAT (in red) methods. The conformation for the transition state calculated with the G3B3 is also presented in the graph. Bond lengths are given in Angstrom (\AA) while angles are in degrees.

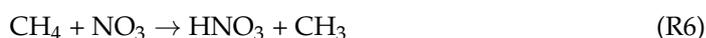
Table 1. Individual contributions (kJ mol^{-1}) of various terms to the total barrier height of the TS calculated at 0 K using the mHEAT-345(Q) method.

Term	Barrier Height
δE_{SCF}	-10.89
$\delta E_{\text{CCSD(T)}}$	81.57
$\delta E_{\text{T(T)}}$	-2.39
$\delta E_{\text{(Q)-T}}$	4.48
δE_{Core}	0.00
δE_{Scalar}	-0.07
δE_{ZPE}	2.85
δE_{DBOC}	1.14
$\delta E_{\text{Spin-orbit}}$	0.00
mHEAT	76.69 ± 2

To feed our discussion on the H atom abstraction efficiency of NO_3 , it is interesting to compare the energy barrier of reaction (R4) with those of (R5) and (R6), where a hydrogen atom of H_2 has been substituted by a Cl atom in (R5) and a CH_3 group in (R6) (Table 2):



with $\Delta_r H^\circ (298 \text{ K}) = 6 \text{ kJ mol}^{-1}$ [13].



with $\Delta_r H^\circ (298 \text{ K}) = 13.7 \text{ kJ mol}^{-1}$ [13].

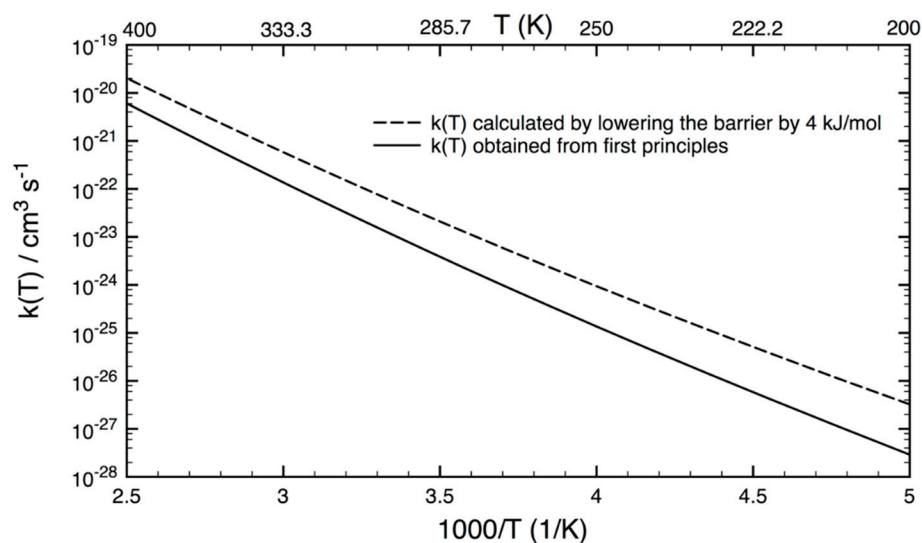
Table 2. Thermochemical values ($\Delta_r H^\circ$), energy barriers (V_a), and rate coefficients (k) for reactions (R4), (R5), and (R6).

Reaction	$\Delta_r H^\circ$ (0 K) in kJ mol^{-1}		V_a (kJ mol^{-1})	k (298 K) $\text{cm}^3 \text{s}^{-1}$
	ATcT	G3B3		
$\text{H}_2 + \text{NO}_3 \rightarrow \text{HNO}_3 + \text{H}$	12.2 ± 0.3	12.8	(76.7 ^a), 74.6 ^b	$<10^{-22}$ ^a
$\text{HCl} + \text{NO}_3 \rightarrow \text{HNO}_3 + \text{Cl}$	7.7 ± 0.5	1.31	57.4 ^b	$<5 \times 10^{-17}$ ^c
$\text{CH}_4 + \text{NO}_3 \rightarrow \text{HNO}_3 + \text{CH}_3$	12.5 ± 0.3	8.2	52.2 ^b	2×10^{-20} ^d

^a: Theory: this work calculated with the mHEAT method, ^b: Theory: calculated with the G3B3 method, ^c: Experimental upper limit is given by Atkinson et al. [43], ^d: Experimentally determined value by Zhou et al. [44].

As seen in Table 2, the H–Cl bond strength is weaker than that of the H–H bond, and the energy barrier of the H-abstraction from HCl by NO_3 radical is calculated to be ca. 57.4 kJ mol^{-1} smaller than the reaction (R4), as expected. In the case of (R6), the energy barrier was calculated to be 52.2 kJ mol^{-1} , lower than the reaction (R4), although the H– CH_3 bond strength is nearly equal to that of the H–H. This is because CH_3 is an electron donor group, and thus the H-abstraction process by the electrophilic NO_3 radical can easily take place. For the three reactions considered here, the H-abstraction of a H atom of H_2 by NO_3 has the highest barrier; therefore, the title reaction rate constant is the slowest, as expected.

Figure 2 shows the reaction rate constants calculated from first principles (the solid line) using the non-separable SCTST theory, while the dashed line represents the results obtained after lessening the barrier by 4 kJ mol^{-1} , which is assumed to be the maximum error produced with the mHEAT method in this case. As seen there, the calculated rate constants increase with temperature, as expected, from $10^{-27} \text{ cm}^3 \text{ s}^{-1}$ at 200 K rising to $10^{-20} \text{ cm}^3 \text{ s}^{-1}$ at 400 K. So, the title reaction is too slow to be important. Unfortunately, there are no experimental data to have a close comparison between the two. According to Figure 2, at 298 K, an upper limit of $10^{-22} \text{ cm}^3 \text{ s}^{-1}$ can be proposed for the title reaction rate constant. Therefore, a consuming frequency of $<5.0 \times 10^{-4} \text{ s}^{-1}$ for the reaction of NO_3 with H_2 can be derived using an average $[\text{NO}_3] = 5.0 \times 10^8 \text{ cm}^{-3}$. This value is about five orders of magnitude slower than the reaction of OH with H_2 (ca. 60 s^{-1} with $[\text{OH}] = 10^6 \text{ cm}^{-3}$). Therefore, the NO_3 -initiated degradation of H_2 is negligibly slow as compared to OH, and thus it has a limited atmospheric impact.

**Figure 2.** Calculated rate constants ($\text{cm}^3 \text{ s}^{-1}$) of the title reaction in the atmospheric temperature range of 200 to 400 K. The solid line represents the results from first principles while the dashed line shows the results obtained when lowering the barrier height by 4 kJ mol^{-1} .

4. Conclusions

The reaction mechanism, thermochemistry, and kinetics of the title reaction have been investigated for the first time to estimate the atmospheric loss of H₂ via reacting with NO₃ radicals. The potential energy surface was constructed using high-accuracy composite G3B3 and mHEAT methods, which can provide an accuracy of about 4 kJ mol⁻¹ for the barrier height in this case. The reaction mechanism was determined, and it was found to undergo a direct H-abstraction process via a barrier height of 76 ± 4 kJ mol⁻¹ leading to HNO₃ plus H atom. The succeeding statistical kinetics analysis based on non-separable SCTST theory generated an analytical expression of $k(T) = 10^{-15} \times T^{0.7} \times \exp\left(-\frac{6120}{T}\right)$ (cm³ s⁻¹) for the reaction rate constants in a temperature range of 200–400 K. The sink of H₂ through reacting with NO₃ radicals was identified to be insignificant in the Earth's atmosphere. And thus, dry deposition and removal by OH radicals are the dominant sinks of H₂ in the atmosphere. It is therefore concluded that the impacts of the title reaction to the climate are probably also negligible. However, to provide safer conclusions, it is necessary to introduce the current results in climate models.

Supplementary Materials: The following supporting information can be downloaded at: <https://www.mdpi.com/article/10.3390/atmos13081313/s1>, Optimized geometries of various species in the H₂ + NO₃ reaction using G3B3 theory.

Author Contributions: M.N.R. conceived the presented ideas. M.N.R. and T.L.N. performed the computations. All authors have read and agreed to the published version of the manuscript.

Funding: This work is part of the Labex CaPPA project funded by ANR through the PIA under contract ANR-11-LABX-0005-01, the "Hauts-de-France" Regional Council, and the European Regional Development Fund (ERDF).

Institutional Review Board Statement: Not applicable.

Informed Consent Statement: Not applicable.

Data Availability Statement: Not applicable.

Acknowledgments: T.L.N. thanks the Department of Chemistry, the University of Florida for the financial support.

Conflicts of Interest: The authors declare no conflict of interest.

References

1. Zhongming, Z.; Linong, L.; Xiaona, Y.; Wangqiang, Z.; Wei, L. Intergovernmental Panel on Climate Change (IPCC) Report. 2021. Available online: <https://www.unep.org/resources/report/climate-change-2021-physical-science-basis-working-group-i-contribution-sixth> (accessed on 25 July 2022).
2. Lelieveld, J.; Pozzer, A.; Pöschl, U.; Fnais, M.; Haines, A.; Münzel, T. Loss of life expectancy from air pollution compared to other risk factors: A worldwide perspective. *Cardiovasc. Res.* **2020**, *116*, 1910–1917. [[CrossRef](#)] [[PubMed](#)]
3. European Commission; Directorate General for Research. *Hydrogen Energy and Fuel Cells: A Vision of Our Future: Final Report of the High Level Group*; Official Publications of the European Communities: Luxembourg, 2003; ISBN 92-894-5589-6.
4. Kleijn, R.; van der Voet, E. Resource constraints in a hydrogen economy based on renewable energy sources: An exploration. *Renew. Sustain. Energy Rev.* **2010**, *14*, 2784–2795. [[CrossRef](#)]
5. Tromp, T.K.; Shia, R.-L.; Allen, M.; Eiler, J.M.; Yung, Y.L.J.S. Potential environmental impact of a hydrogen economy on the stratosphere. *Science* **2003**, *300*, 1740–1742. [[CrossRef](#)] [[PubMed](#)]
6. Schultz, M.G.; Diehl, T.; Brasseur, G.P.; Zittel, W. Air pollution and climate-forcing impacts of a global hydrogen economy. *Science* **2003**, *302*, 624–627. [[CrossRef](#)] [[PubMed](#)]
7. Prather, M.J. An environmental experiment with H₂? *Science* **2003**, *302*, 581–582. [[CrossRef](#)]
8. Warwick, N.J.; Bekki, S.; Nisbet, E.G.; Pyle, J.A. Impact of a hydrogen economy on the stratosphere and troposphere studied in a 2-D model. *Geophys. Res. Lett.* **2004**, *31*, L05107. [[CrossRef](#)]
9. Wang, D.; Jia, W.; Olsen, S.C.; Wuebbles, D.J.; Dubey, M.K.; Rockett, A.A. Impact of a future H₂-based road transportation sector on the composition and chemistry of the atmosphere—Part 2: Stratospheric ozone. *Atmos. Chem. Phys.* **2013**, *13*, 6139–6150. [[CrossRef](#)]
10. Ehhalt, D.H.; Rohrer, F. The tropospheric cycle of H₂: A critical review. *Tellus B Chem. Phys. Meteorol.* **2009**, *61*, 500–535. [[CrossRef](#)]

11. Novelli, P.C.; Lang, P.M.; Masarie, K.A.; Hurst, D.F.; Myers, R.; Elkins, J.W. Molecular hydrogen in the troposphere: Global distribution and budget. *J. Geophys. Res. Atmos.* **1999**, *104*, 30427–30444. [[CrossRef](#)]
12. Patterson, J.D.; Aydin, M.; Crotwell, A.M.; Pétron, G.; Severinghaus, J.P.; Krummel, P.B.; Langenfelds, R.L.; Saltzman, E.S. H₂ in Antarctic firn air: Atmospheric reconstructions and implications for anthropogenic emissions. *Proc. Natl. Acad. Sci. USA* **2021**, *118*, e2103335118. [[CrossRef](#)]
13. Ruscic, B.; Bross, D.H. Active Thermochemical Tables (ATcT) Values Based on Ver. 1.122r of the Thermochemical Network. Available online: ATcT.anl.gov (accessed on 4 July 2022).
14. Burkholder, J.B.; Sander, S.P.; Abbatt, J.P.D.; Barker, J.R.; Cappa, C.D.; Crouse, J.D.; Dibble, T.S.; Huie, R.E.; Kolb, C.E.; Kyrilo, M.J.; et al. *Chemical Kinetics and Photochemical Data for Use in Atmospheric Studies Evaluation Number 19*; Jet Propulsion Laboratory, National Aeronautics and Space: Pasadena, CA, USA, 2020.
15. Wang, X.; Jacob, D.J.; Eastham, S.D.; Sulprizio, M.P.; Zhu, L.; Chen, Q.; Alexander, B.; Sherwen, T.; Evans, M.J.; Lee, B.H. The role of chlorine in global tropospheric chemistry. *Atmos. Chem. Phys.* **2019**, *19*, 3981–4003. [[CrossRef](#)]
16. Finlayson-Pitts, B.J.; Pitts, J.N. (Eds.) *Chemistry of the Upper and Lower Atmosphere*; Academic Press: San Diego, CA, USA, 2000; pp. 86–129.
17. Farman, J.C.; Gardiner, B.G.; Shanklin, J.D. Large losses of total ozone in antarctica reveal seasonal ClO_x/NO_x interaction. *Nature* **1985**, *315*, 207–210. [[CrossRef](#)]
18. Wayne, R.P.; Barnes, I.; Biggs, P.; Burrows, J.P.; Canosa-Mas, C.E.; Hjorth, J.; le Bras, G.; Moortgat, G.K.; Perner, D.; Poulet, G. The nitrate radical—physics, chemistry, and the atmosphere. *Atmos. Environ. Part A Gen. Top.* **1991**, *25*, 1–203. [[CrossRef](#)]
19. Ng, N.L.; Brown, S.S.; Archibald, A.T.; Atlas, E.; Cohen, R.C.; Crowley, J.N.; Day, D.A.; Donahue, N.M.; Fry, J.L.; Fuchs, H. Nitrate radicals and biogenic volatile organic compounds: Oxidation, mechanisms, and organic aerosol. *Atmos. Chem. Phys.* **2017**, *17*, 2103–2162. [[CrossRef](#)] [[PubMed](#)]
20. Appel, B.R.; Wall, S.M.; Tokiwa, Y.; Haik, M. Simultaneous nitric-acid, particulate nitrate and acidity measurements in ambient air. *Atmos. Environ.* **1980**, *14*, 549–554. [[CrossRef](#)]
21. Galloway, J.N.; Likens, G.E. Acid precipitation—the importance of nitric acid. *Atmos. Environ.* **1981**, *15*, 1081–1085. [[CrossRef](#)]
22. Frisch, M.J.; Trucks, G.W.; Schlegel, H.B.; Scuseria, G.E.; Robb, M.A.; Cheeseman, J.R.; Scalmani, G.; Barone, V.; Petersson, G.A.; Nakatsuji, H.; et al. Gaussian Software Package, 2009, for Quantum Chemical Calculations. Available online: https://www.researchgate.net/publication/260433987_Gaussian_09_Revision_A02 (accessed on 25 July 2022).
23. Baboul, A.G.; Curtiss, L.A.; Redfern, P.C.; Raghavachari, K. Gaussian-3 theory using density functional geometries and zero-point energies. *J. Chem. Phys.* **1999**, *110*, 7650–7657. [[CrossRef](#)]
24. Curtiss, A.; Raghavachari, K.; Redfern, P.C.; Rassolov, V.; Pople, J.A. Gaussian-3 (G3) theory for molecules containing first and second-row atoms. *J. Chem. Phys.* **1998**, *109*, 7764–7776. [[CrossRef](#)]
25. Francl, M.M.; Pietro, W.J.; Hehre, W.J.; Binkley, J.S.; Gordon, M.S.; DeFrees, D.J.; Pople, J.A. Self-consistent molecular-orbital methods. 23. A polarization-type basis set for 2nd-row elements. *J. Chem. Phys.* **1982**, *77*, 3654–3665. [[CrossRef](#)]
26. Nguyen, T.L.; Romanias, M.N.; Ravishankara, A.R.; Zaras, A.M.; Dagaut, P.; Stanton, J.F. The atmospheric impact of the reaction of N₂O with NO₃: A theoretical study. *Chem. Phys. Lett.* **2019**, *731*, 136605. [[CrossRef](#)]
27. Thorpe, J.H.; Lopez, C.A.; Nguyen, T.L.; Baraban, J.H.; Bross, D.H.; Ruscic, B.; Stanton, J.F. A modified recipe for computational efficiency. *J. Chem. Phys.* **2019**, *150*, 224102. [[CrossRef](#)] [[PubMed](#)]
28. Matthews, D.A.; Cheng, L.; Harding, M.E.; Lipparini, F.; Stopkowitz, S.; Jagau, T.-C.; Szalay, P.G.; Gauss, J.; Stanton, J.F. Coupled-cluster techniques for computational chemistry: The CFOUR program package. *J. Chem. Phys.* **2020**, *152*, 214108. [[CrossRef](#)] [[PubMed](#)]
29. Miller, W.H. Semiclassical Theory for Non-Separable Systems—Construction of Good Action-Angle Variables for Reaction-Rate Constants. *Faraday Discuss. Chem. Soc.* **1977**, *62*, 40–46. [[CrossRef](#)]
30. Miller, W.H.; Hernandez, R.; Handy, N.C.; Jayatilaka, D.; Willetts, A. Abinitio Calculation of Anharmonic Constants for a Transition-State, with Application to Semiclassical Transition-State Tunneling Probabilities. *Chem. Phys. Lett.* **1990**, *172*, 62–68. [[CrossRef](#)]
31. Hernandez, R.; Miller, W.H. Semiclassical Transition-State Theory—a New Perspective. *Chem. Phys. Lett.* **1993**, *214*, 129–136. [[CrossRef](#)]
32. Nguyen, T.L.; Barker, J.R. Sums and Densities of Fully Coupled Anharmonic Vibrational States: A Comparison of Three Practical Methods. *J. Phys. Chem. A* **2010**, *114*, 3718–3730. [[CrossRef](#)] [[PubMed](#)]
33. Nguyen, T.L.; Stanton, J.F.; Barker, J.R. Ab Initio Reaction Rate Constants Computed Using Semiclassical Transition-State Theory: HO + H₂ → H₂O + H and Isotopologues. *J. Phys. Chem. A* **2011**, *115*, 5118–5126. [[CrossRef](#)] [[PubMed](#)]
34. Miller, W.H. Tunneling Corrections to Unimolecular Rate Constants, with Application to Formaldehyde. *J. Am. Chem. Soc.* **1979**, *101*, 6810–6814. [[CrossRef](#)]
35. Bowman, J.M. Reduced Dimensionality Theory of Quantum Reactive Scattering. *J. Phys. Chem.* **1991**, *95*, 4960–4968. [[CrossRef](#)]
36. Balakrishnan, N. Quantum mechanical investigation of the O + H₂ → OH + H reaction. *J. Chem. Phys.* **2003**, *119*, 195–199. [[CrossRef](#)]
37. Wang, F.G.; Landau, D.P. Efficient, multiple-range random walk algorithm to calculate the density of states. *Phys. Rev. Lett.* **2001**, *86*, 2050–2053. [[CrossRef](#)] [[PubMed](#)]

38. Wang, F.G.; Landau, D.P. Determining the density of states for classical statistical models: A random walk algorithm to produce a flat histogram. *Phys. Rev. E* **2001**, *64*, 056101. [[CrossRef](#)] [[PubMed](#)]
39. Basire, M.; Parneix, P.; Calvo, F. Quantum anharmonic densities of states using the Wang-Landau method. *J. Chem. Phys.* **2008**, *129*, 081101. [[CrossRef](#)] [[PubMed](#)]
40. Nguyen, T.L.; Stanton, J.F.; Barker, J.R. A practical implementation of semi-classical transition state theory for polyatomics. *Chem. Phys. Lett.* **2010**, *499*, 9–15. [[CrossRef](#)]
41. Baer, T.; Hase, W.L. *Unimolecular Reaction Dynamics: Theory and Experiments*; Oxford University Press: New York, NY, USA, 1996.
42. Sander, S.P.; Friedl, R.R.; Barker, J.R.; Golden, D.M.; Kurylo, M.J.; Wine, P.H.; Abbatt, J.P.D.; Burkholder, J.B.; Kolb, C.E.; Moorgat, G.K. Jet Propulsion Laboratory (JPL) Science. Available online: <https://science.jpl.nasa.gov/> (accessed on 4 July 2022).
43. Atkinson, R.; Baulch, D.L.; Cox, R.A.; Crowley, J.N.; Hampson, R.F.; Hynes, R.G.; Jenkin, M.E.; Rossi, M.J.; Troe, J. Evaluated kinetic and photochemical data for atmospheric chemistry: Volume III—Gas phase reactions of inorganic halogens. *J. Atmos. Chem. Phys.* **2007**, *7*, 981–1191. [[CrossRef](#)]
44. Zhou, L.; Ravishankara, A.R.; Brown, S.S.; Zarzana, K.J.; Idir, M.; Daële, V.; Mellouki, A. Kinetics of the reactions of NO₃ radical with alkanes. *Phys. Chem. Chem. Phys.* **2019**, *21*, 4246–4257. [[CrossRef](#)]